Journal of Alloys and Compounds 509 (2011) 7663–7670

Contents lists available at ScienceDirect

Journal of Alloys and Compounds

journal homepage: www.elsevier.com/locate/jallcom

Electrical and switching properties of $Se_{85}Te_{15-x}Sb_x$ ($0 \leq x \leq 6$ at.wt%) thin films

M. Fadel [a], N.A. Hegab [a], I.S. Yahia [a], A.M. Salem [b], A.S. Farid [a,*]

[a] Physics Department, Faculty of Education, Ain Shams University, Cairo, Egypt
[b] Physics Division, Electron Microscopy and Thin Film Laboratory, National Research Center, Dokki, Cairo, Egypt

ARTICLE INFO

Article history:
Received 2 October 2010
Received in revised form 12 April 2011
Accepted 16 April 2011
Available online 23 April 2011

Keywords:
Amorphous chalcogenide semiconductors
Se–Te–Sb alloys
Memory switching
Threshold voltage
Electrothermal model

ABSTRACT

Thin film samples of different thicknesses ranging from 167.5 to 647.4 nm, were prepared from the synthesized amorphous $Se_{85}Te_{15-x}Sb_x$ ($x = 0$, 2, 4 and 6 at.wt%) chalcogenide glass compositions by thermal evaporation technique. X-ray diffraction analysis showed the amorphous nature of the obtained films. The dc electrical conductivity was studied for the prepared films as a function of temperature in range (297–333 K) below the glass transition temperature T_g. From the obtained results of σ_{dc} the conduction activation energy ΔE_σ has a single value indicating the presence of one conduction mechanism throughout the studied range of temperature. The obtained results of σ_{dc} are explained in accordance with Mott and Davis model. The current–voltage (I–V) characteristics curves showed a memory type switch. The mean value of the threshold voltage $\bar{V}_{th}$ increases linearly with increasing film thickness and decreases exponentially with temperature for all investigated film compositions. Values of the threshold voltage activation energy $\bar{\varepsilon}_{V_{th}}$ were obtained for the studied films. The switching phenomenon in the investigated films is explained on the basis of the electrothermal model initiated from Joule heating of current channel. The effect of the Sb addition on the obtained results was discussed.

1. Introduction

In recent years, chalcogenide glasses have received a lot of attention because of their potential and current use in various solid-state optical and electrical devices. Both selenium and tellurium are expected to be the important semiconductor elements, because of their possible application in the fabrication of semiconductor devices.

Amorphous selenium has been emerged as promising material because of its interesting electrical applications. It is widely preferred in the fabrication of electro photographic devices and switching and memory devices [1]. The shortcoming of amorphous selenium (a-Se) for use in photographic drum such as its short life time and low sensitivity, can be overcome by the use of certain additives like Ge, Te, Bi, Sb, In, etc. The use of binary alloys has been of great interest for their greater hardiness, higher sensitivity, higher crystallization and smaller aging effect as compared to amorphous selenium [2]. Because of these advantages these alloys are nowdays preferred in various solid state devices. The properties of a-Se and the effect of alloying Te into a-Se have been studied by various workers [3–5].

Glassy alloys of Se–Te system based on Se have become materials of considerable commercial, scientific and technological importance. They are widely used for various applications in many fields as optical recording media because of their excellent laser writer sensitivity, Xerography, and electrographic applications such as photoreceptors in photocopying and laser printing [6–8]. It is found that the properties of chalcogenide semiconductors are usually affected by the addition of impurities as third element. The incorporation of third element in binary chalcogenide glassy alloys is necessary to get relatively stable glassy alloys, and leads to enlarge their domain of applications. From this point of view, the addition of Sb to Se–Te binary system can markedly affect its structural, electrical and optical properties [9–13]. Studies of these properties and others are believed to be useful for improving the stability characteristics of the devices based on Se–Te–Sb films. The addition of Sb to the chalcogenide glasses expands the glass forming area and also creates compositional and configurational disorder in the system [14–16].

The switching property of chalcogenide glasses is probably their electrical switching, discovered by Ovshinsky in 1968 [17], which has found applications in the areas such as information storage [18], power control devices, thermistors, etc. [19]. There are two types of electrical switching observed in these materials, namely threshold and memory type. In the threshold type switching, the ON-state persists only while the current flows down to a certain holding voltage, whereas in memory-type switching, the ON-state is permanent until a suitable rest current pulse is applied across the sample. Different mechanisms have been proposed to explain the electrical switching in chalcogenide glasses. These include pure electronic

* Corresponding author. Tel.: +20 180247160; fax: +20 2 22581243.
E-mail address: abir_net_2005@hotmail.com (A.S. Farid).

0925-8388/$ – see front matter © 2011 Elsevier B.V. All rights reserved.
doi:10.1016/j.jallcom.2011.04.093

[20] electrothermal [21] and thermal [9,22] mechanisms. It is more or less accepted that threshold switching is generally electronic in origin, whereas as the memory switching is of thermal in origin [9,23]. The formation of highly conductive crystalline channels (or filaments) is considered as a possible cause of memory switching in chalcogenide glasses [24,25].

The present paper aims to study:(1) the dc electrical conductivity of $Se_{85}Te_{15-x}Sb_x$ (x = 0, 2, 4 and 6 at.wt%). (2) The switching phenomenon, the parameters affecting the threshold switching voltage and identifying the suitable switching mechanism for switching process. (3) The effect of Sb addition on the dc electrical conductivity and switching properties.

2. Experimental details

$Se_{85}Te_{15-x}Sb_x$ (x = 0, 2, 4 and 6 at.wt%) compositions were synthesized as follows: the elementary constituents of each composition of purity 99.999% were weighted in accordance with their atomic percentage and loaded in a silica tube. Tubes with their constituent elements (5 g total weight) were sealed under vacuum of 10^{-5} Torr. The tube is placed in an oscillatory furnace and heated stepwise by a rate 5 K/min at 1123 K to allow Se, Te and Sb to react completely. The ampoule was frequently rocked for 12 h at the maximum temperature to make the melt homogenous. The quenching was performed in ice water and then the alloy was taken out by cutting the tube. The initial vitreous alloys were powdered and separated according to the size.

Thin films of the different compositions of $Se_{85}Te_{15-x}Sb_x$ (x = 0, 2, 4 and 6 at.wt%) were prepared by the thermal evaporation method under vacuum (10^{-5} Torr) on to cleaned glass substrates (for electrical measurements), and highly polished pyrographite substrates (for switching measurements). The film thickness was measured using the thickness monitor (Edwards, FTM5) and confirmed after deposition by Tolansky's interferometric method [26].

The chemical composition of the investigated samples was checked by energy dispersive X-ray analysis (EDX) using JOEL 5400 scanning electron microscope. The structural identification of the investigated compositions in thin film form was confirmed by both X-ray diffraction XRD using Philips X-ray unit (PW-3710) with generator (PW-1830) Supplied with a copper target with Ni filter. The X-ray tube was operated at 40 kV and 30 mA. Glass transition temperature obtained using differential scanning calorimetry (DSC) (Shimadzu DSC-50).

For dc electrical conductivity, the prepared films were sandwiched between two Al electrodes and measured through a special designed holder. The electrode contacts were of an ohmic nature as determined by dc conductivity study. An electrometer of the type (Keithly E-616A) was used for measurements of resistivity in the temperature range (297–333 K). The dc conductivity was calculated according to the relation $\sigma_{dc} = d/RA$ where R is the resistance of the sample, d is the sample thickness and A is the cross-sectional areas of the sample.

Switching phenomenon was investigated for the prepared $Se_{85}Te_{15-x}Sb_x$ film compositions. Measurements of the I–V characteristics were carried out in an especially constructed measuring cell of two electrodes [10]. The film sample deposited on a pyrographite substrate is placed on the lower copper electrode. The lower electrode was a circular brass disk in contact with the pyrogaphite substrate and the upper one was a movable platinum wire with a thin circular end of diameter 2×10^{-4} m which connected by a weak spring to provide a gentle and good contact with the upper surface of the film. The pressure provided by the upper electrode as well as the point contact was kept constant throughout the measurements. The measuring cell was introduced in a simple electrical circuit provided with a digital electrometer (Keithley E-616A) and a sensitive digital multimeter to measure the respective potential drop and the current (as low as 10^{-9} A) passing through the sample. These measurements were made at room temperature as well as at elevated temperatures using a heating system and the sample temperature was determined using a chromel–alumel thermocouple in close to the sample.

3. Results and discussion

3.1. Structure identification of $Se_{85}Te_{15-x}Sb_x$ (x = 0, 2, 4 and 6 at.wt%)

3.1.1. X-ray characterization

X-ray diffraction was carried out for the investigated compositions in thin film form. The obtained patterns are illustrated in Fig. 1. This figure revealed that there is no evidence peak, ensuring that the structure of the prepared films is of amorphous nature. The same behavior was obtained for all other films.

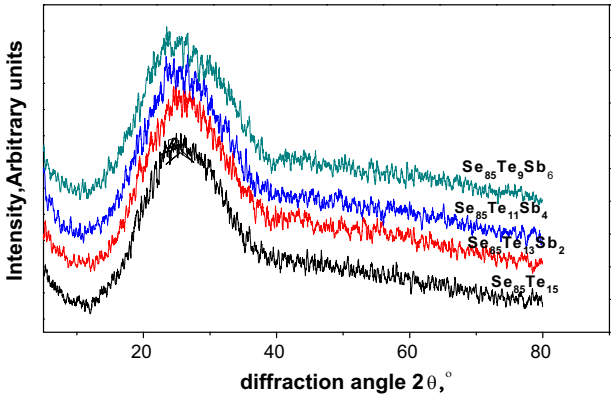

Fig. 1. X-ray diffraction patterns for $Se_{85}Te_{15-x}Sb_x$ (x = 0, 2, 4 and 6 at%) films of nearly the same thickness.

3.1.2. Differential scanning calorimetry (DSC)

When the sample is heated at a constant rate in a differential scanning calorimetry experiment the glass undergoes structural changes. The scanning character of DSC provides as thermal spectrum of characteristic transitions such as glass transitions (endothermic peak T_g), crystallization peak T_c (exothermic peak), and the third transition is melting which of course endothermic peak. The T_g value for glassy materials indicates a transition from a rigid to flexible, which causes a change in heat capacity structure and hence there is a shift in base line. So, all measurements in the present study were carried out at temperature less than the corresponding T_g for each composition. Fig. 2 shows a typical DSC thermograms of $Se_{85}Te_{15-x}Sb_x$ (x = 0, 2, 4 and 6 at.wt%) glassy samples at a heating rate 10 °C/min. It is clear from this figure that all samples showed a single glass transition and crystallization, which confirms the homogeneity of the samples. The obtained values of the glass transition temperature T_g of samples under test are listed in Table 1.

It is clear from this table that T_g increases with Sb up to 4 at.wt% then decreases as Sb content increases. The variation of the glass transition temperature T_g of these glasses can be explained on the basis of structural changes due to the introduction of Sb atoms. It

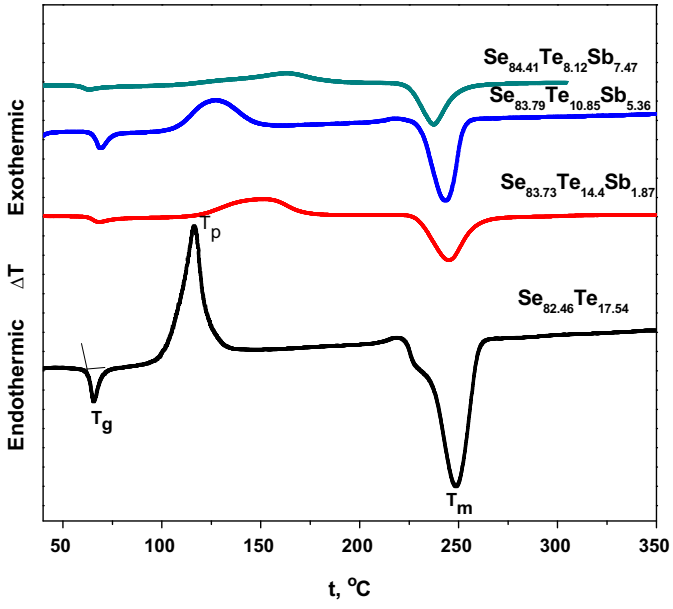

Fig. 2. Differential scanning calorimetry for the investigated compositions in a powder form.

Table 1
Values of T_g, and bond energy values for bonds in $Se_{85}Te_{15-x}Sb_x$ films.

Composition	T_g, K^{-1}	Bond	Bond energy, kJ/mole
$Se_{85}Te_{15}$	61.8	Se–Se	189.22
$Se_{85}Te_{13}Sb_2$	62.9	Te–Te	142.35
$Se_{85}Te_{11}Sb_4$	64.6	Se–Te	187.57
$Se_{85}Te_9Sb_6$	58.1	Se–Sb	214.20
		Sb–Sb	176.40

is known that a-Se about 40% of the atoms have a ring structure and 60% of the atoms are bonded as polymeric chains. Tellurium enters as copolymer chains and tends to reduce the number of Se_8 rings [27]. Simultaneously, it increases the number of Se and Te atoms in the chains. The structure of Se–Te system prepared by quenching the melt is regarded as a mixture of Se_8 rings, Se_6Te_2 rings and Se–Te copolymer chains. A strong covalent bond exists between the atoms in the ring whereas in between chains only Vander Wall's forces are dominant [28]. The addition of Sb with small amounts (2–4 at.wt%) to Se–Te system leads to its entry into the cross-link chains, and Se–Sb bonds with higher bond energy (214.2 kJ/mole) are formed, replacing the Te–Sb bond which have lower bond energy (205.8 kJ/mole) see Table 1 [11], i.e. Se_8 ring decreases. As a result the glassy matrix becomes heavily cross-linked and the steric hindrance increases makes the structure more rigid. Since T_g reflects the rigidity of the structure [29], it is expected that T_g increases with increasing Sb content (2–4 at.wt%). Further addition of Sb (Sb > 4 at.wt%) leads to the formation of Sb–Sb bonds (bond energy 176.4 kJ/mole) resulting in decreasing the Se–Sb bond concentration and the concentration of Se_8 rings increases in the glass matrix. The decrease of T_g leads to the increasing of the ring concentration, this in turn explains the decrease in T_g value with the increase of Sb content higher than 4 at.wt% [11]. The obtained glasses are stable up to 4 at.wt% of Sb content and increasing Sb content leads to the lower of the system stability.

3.1.3. Electron dispersive X-ray spectrum analysis EDX

Composition of the investigated films was checked by energy dispersive X-ray spectrum analysis using a scanning electron microscope. The obtained data showed that the percentage of the constituent elements of the studied compositions are approximately the same as tabulated in Table 2.

3.2. Dc electrical conductivity

The dc electrical conductivity σ_{dc} was measured for the studied film compositions in the temperature range (297–333 K) and in thickness range (167.5–432 nm). The narrow temperature range of the present measurements is due to the low glass transition temperature. Fig. 3a–d shows the temperature dependence of σ_{dc} for the studied film compositions. From this figure, $\ln \sigma_{dc}$ versus $1000/T$ curves are straight lines in the considered temperature and thickness ranges. This indicates that the conduction in these glasses is

Table 2
EDX for $Se_{85}Te_{15-x}Sb_x$ films.

Calculated composition	At % (observed)			Nominal compositions
	Se	Te	Sb	
$Se_{85}Te_{15}$	82.46	17.54	–	$Se_{82.46}Te_{17.54}$
$Se_{85}Te_{13}Sb_2$	83.73	14.40	1.87	$Se_{83.73}Te_{14.4}Sb_{1.87}$
$Se_{85}Te_{11}Sb_4$	83.79	10.85	5.36	$Se_{83.79}Te_{10.85}Sb_{5.36}$
$Se_{85}Te_9Sb_6$	84.41	8.12	7.47	$Se_{84.41}Te_{8.12}Sb_{7.47}$

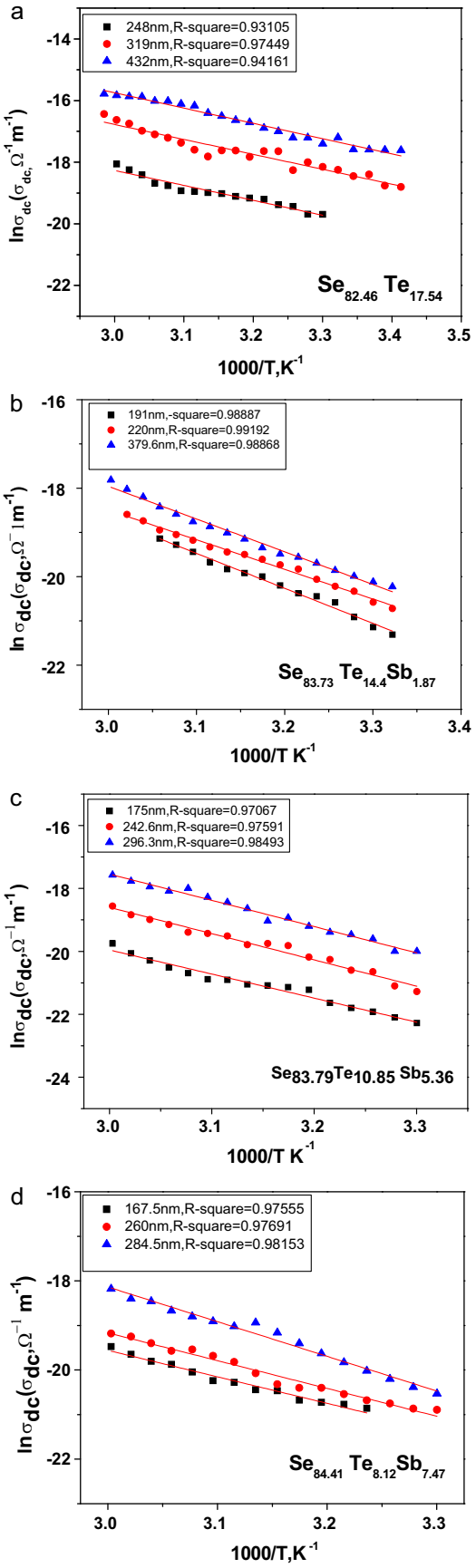

Fig. 3. (a–d) Temperature dependence of dc-electrical conductivity for of $Se_{85}Te_{15-x}Sb_x$ (x = 0, 2, 4 and 6 at%) film compositions at different thicknesses.

Table 3
Values of σ_{RT}, σ_o, ΔE_σ for $Se_{85}Te_{15-x}Sb_x$ films.

Composition	σ_{RT}, $(\Omega\,m)^{-1}$	ΔE_σ, eV	σ_o, $(\Omega\,m)^{-1}$
$Se_{85}Te_{15}$	2.68×10^{-9}	0.58	8.2×10^{-3}
$Se_{85}Te_{13}Sb_2$	1.15×10^{-9}	0.72	1.59×10^{-3}
$Se_{85}Te_{11}Sb_4$	3.85×10^{-10}	0.825	2.38×10^{-3}
$Se_{85}Te_9Sb_6$	8.72×10^{-10}	0.618	5.31×10^{-4}

through an activated process. The σ_{dc} can, therefore, be expressed by the well known relation:

$$\sigma = \sigma_o \exp\left(\frac{-\Delta E_\sigma}{k_B T}\right), \quad (1)$$

where σ_o is the pre-exponential factor, k_B is the Boltzmann constant, T is the absolute temperature and ΔE_σ is the conduction activation energy. It is clear that the obtained relations are straight lines which have single value of activation energy, i.e. there is one type of conduction mechanism contributing to the dc conductivity.

Values of ΔE_σ are calculated from the slopes of the lines of Fig. 3a–d according to Eq. (1) and tabulated in Table 3 together with the room temperature conductivity σ_{RT}. The values of σ_o, which calculated as the intercept at $T^{-1} = 0$ of Fig. 3a–d for all films (see Table 2). From Table 2, it was suggested that the values of σ_o assumed that the conduction mechanism of dc electrical conductivity may be due to hopping of charge carriers between localized at the band edges as suggested by Mott and Davis [12,13]. This mechanism of conduction is familiar in amorphous materials [12,13].

It is found that the values of the activation energy for all the studied samples are thickness independent through the measured range, since the straight lines are parallel. It is also observed that the dc electrical conductivity increases with increasing film thickness. This is because the density of lattice defects as vacancies, interstitials and dislocations, developed through film deposition are lowered during the increase of film thickness and thus, film resistance is decreased and the conductivity is increased with the film thickness.

It is observed from Table 3 that σ_{dc} decreases with a corresponding increase in ΔE_σ with Sb addition up to 4 at.wt% in the studied compositions. This may be due to the enhancement in the network rigidity of the studied compositions resulting in a decrease in σ_{dc}. Further increase of Sb content (Sb > 4 at.wt%) making the structure of the studied films less amorphous (less rigid) thus σ_{dc} increase.

It is a well-established fact that glasses containing Se have a tendency to form polymerized network and the homopolar bond is qualitatively suppressed [30,31]. The addition of small amount of Sb (2–4 at.wt%) to Se–Te system leads to its entry into the cross link chains and hence increasing the glass stability. This stability of the system increases up to 4 at.wt% of Sb and further increment in atomic weight of Sb lowers the stability of the system. One can infer that the composition $Se_{83.79}Te_{10.85}Sb_{5.36}$ has a maximum density of Sb–Sb bonds. Any further increase of Sb percentage inside the host matrix lowers the stability of the glassy system. For lower concentration of Sb, the Se–Se bonds of lower energy now will be replaced by Se–Sb bonds of high energy (see Table 1) and these bonds causes a decrease in σ_{dc} up to Sb = 4 at.wt% as shown in Fig. 4 [11]. Further addition of Sb favors the formation of Sb–Sb bonds (see Section 3.1.2) and so, the reducing of Se–Sb bonds concentration also resulting the increase of the σ_{dc} and decrease the activation energy [32,33]. This is because the unsaturated bonds produced as a result of insufficient number of atoms in amorphous material form defects in material [12]. Such defects produce the localized states in the band gap of amorphous material, which causes the observed variation in the conductivity of the studied films.

The variation of σ_{dc} can be also explained by the increase in the density of defect states. Such an increase in the density of defect states after incorporation of Sb additive (Sb > 4 at.wt%) may be understood in terms of the electron affinity (EA) of Sb (1.07 eV) as suggested by Onozuka et al. [34]. Se and Te belong to the group VI of the periodic table. When Te (EA = 1.97 eV) is added to Se (EA = 2.02 eV), some of the Te atoms may not be incorporated in chains would act as ionized impurities. Similarly, the addition of Sb will increase the positively charged state, since the electron affinity of Sb is much lower than both Se and Te. So an increase in defect state density after adding Sb >4 at.wt% to binary $Se_{85}Te_{15}$ glass may be understood in terms of lower electron affinity of Sb as compared to Se or Te. This increase in defect state density leads to increase in σ_{dc}.

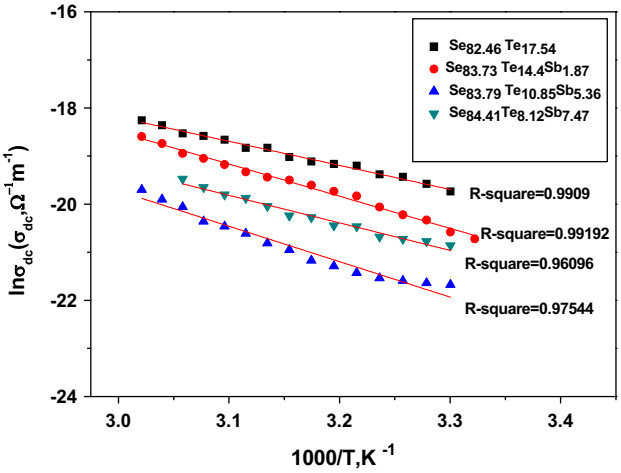

Fig. 4. Temperature dependence of dc-electrical conductivity for $Se_{85}Te_{15-x}Sb_x$ films of nearly the same thickness.

3.3. Switching phenomenon

3.3.1. Current–voltage (I–V) characteristics

The room temperature *I–V* characteristics for the considered compositions were investigated for thin film samples of different thicknesses (167.5–647.4 nm). Fig. 5a and b shows illustrative examples for the *I–V* curve of the $Se_{83.73}Te_{14.4}Sb_{1.87}$ and $Se_{83.79}Te_{10.85}Sb_{5.36}$. It is observed that, with increasing the applied voltage the current increases slowly forming the first branch (*oa*) of the *I–V* curve, called the OFF-state with high resistance. At a certain value of the applied voltage (point *a*), called the threshold switching voltage V_{th}, a sudden increase in the current and consequent decrease in the voltage (point *b*) takes place in a very short time $\sim 10^{-9}$ s, i.e. switching occurs through the load line (*ab*), along which current and voltage readings cannot be recorded. Further increase in the applied voltage, increases the current without significant increase in the potential drop across the sample (part *bc*). This part of the curve representing the ON-state with low resistance. Then, decreasing the applied voltage, the current and voltage decrease to zero value (part *co*) of the curve. If the voltage is further increased and then decreased in the current increases along *oc* then decreases along *co*. It is clear that the obtained curves are typical for a memory switch, which is also obtained for other investigated film compositions of different thicknesses. It must be noted that static *I–V* curves for the investigated film compositions were measured at different points uniformly distributed throughout the whole surface of the film and hence, the mean value of threshold voltage was calculated ($\bar{V}_{th}$).

It has been well understood that memory switching is more probable in chalcogenide glass compositions which will have lower energy barrier for reversible local structural changes [35]. Because of the weaker bonds and flexibility due to the abundance of

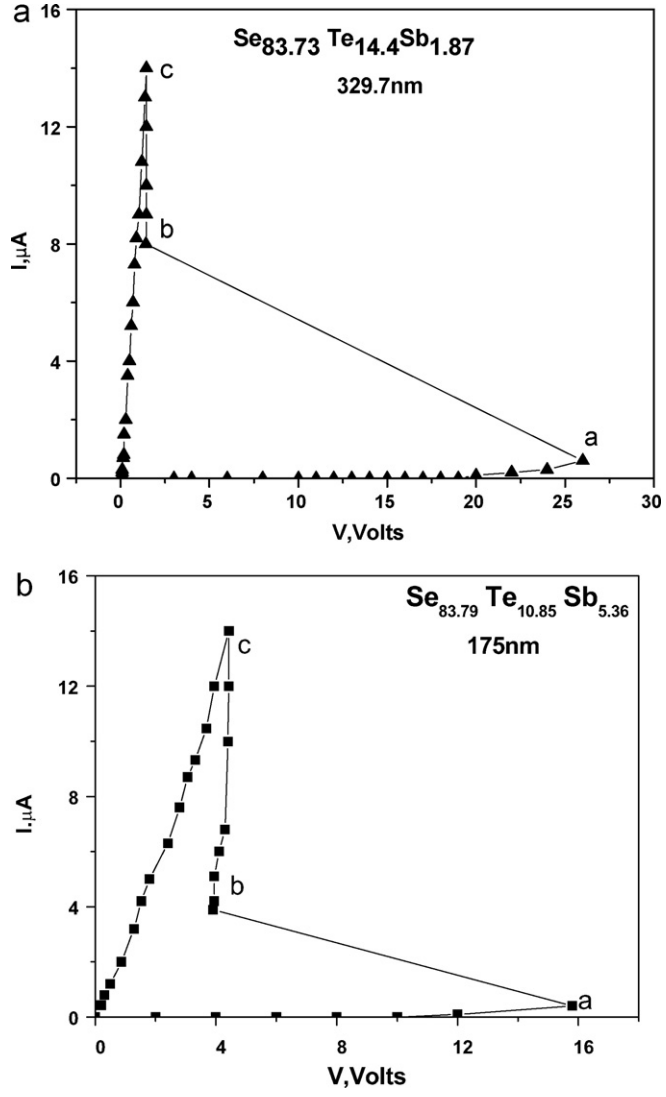

Fig. 5. (a and b) *I–V* characteristic curves for $Se_{83.73}Te_{14.4}Sb_{1.87}$ and $Se_{83.79}Te_{10.85}Sb_{5.36}$ films.

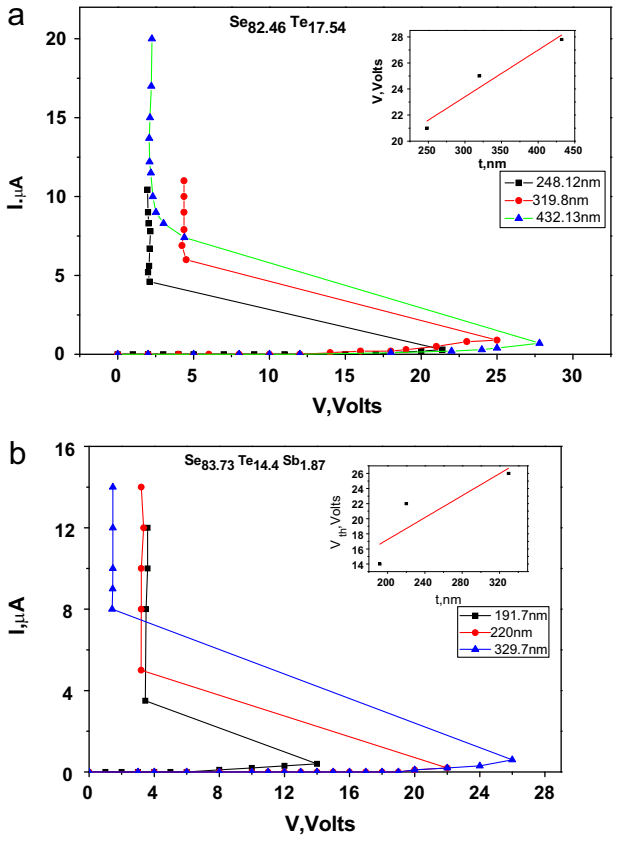

Fig. 6. (a) Room temperature *I–V* characteristic curves of $Se_{82.46}Te_{17.54}$ and $Se_{83.73}Te_{14.4}Sb_{1.87}$. (b) The inset plot of $\bar{V}_{th}$ versus *t*.

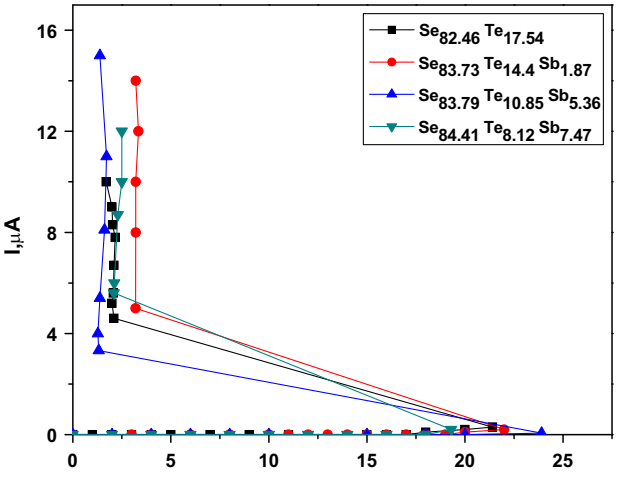

Fig. 7. Room temperature *I–V* characteristic curves of $Se_{85}Te_{15-x}Sb_x$ film compositions of nearly the same thickness.

divalent elements, chalcogenide glasses with low network connectivity/rigidity are more credible for any structural changes [35]. Such floppy glasses [36,37] which will also have lesser thermal stability [38], can permit easy creation of nucleation sites for an extended structural phase changes of the type required for memory switching.

3.3.2. *Thickness dependence of the threshold voltage* $\bar{V}_{th}$

Fig. 6a and b represents the *I–V* curves for $Se_{82.46}Te_{17.54}$ and $Se_{83.73}Te_{14.4}Sb_{1.87}$ films as representative examples as a function of thickness. It is clear that $\bar{V}_{th}$ increases with film thickness, which can be explained by the corresponding increase of film conductance see the inset of the figures. The obtained relation agrees with the results obtained before for other chalcogenide glasses [11,12,33]. Moreover, *I–V* characteristic curves for $Se_{85}Te_{15-x}Sb_x$ ($x = 0, 2, 4$ and 6 at.wt%) are illustrated in Fig. 7. It is clear that the increase of Sb content at the expense of Te content in the studied compositions increases the value of $\bar{V}_{th}$ up to $x = 4$ at.wt% followed by a decrease in $\bar{V}_{th}$ for $x = 6$ at.wt% (see Table 4). This could be understood with respect to the direct relation between $\bar{V}_{th}$ and σ_{dc}, since the latter decrease with Sb content. The obtained increase in $\bar{V}_{th}$ with Sb content up to 4 at.wt% may be explained by the increase of the stronger Se–Sb bonds and further increase of Sb content lead to the decrease

Table 4
Values of V_{th}, $\bar{\varepsilon}_{V_{th}}$, and $\bar{\varepsilon}_{V_{th}}/\Delta E_\sigma$ for $Se_{85}Te_{15-x}Sb_x$ films.

Composition	Thickness, nm	V_{th}, V	$\bar{\varepsilon}_{V_{th}}$, eV	$\bar{\varepsilon}_{V_{th}}/\Delta E_\sigma$
$Se_{85}Te_{15}$	248	21.4	0.29	0.500
$Se_{85}Te_{13}Sb_2$	220	22	0.36	0.500
$Se_{85}Te_{11}Sb_4$	242	23.9	0.41	0.496
$Se_{85}Te_9Sb_6$	260	19.3	0.31	0.500

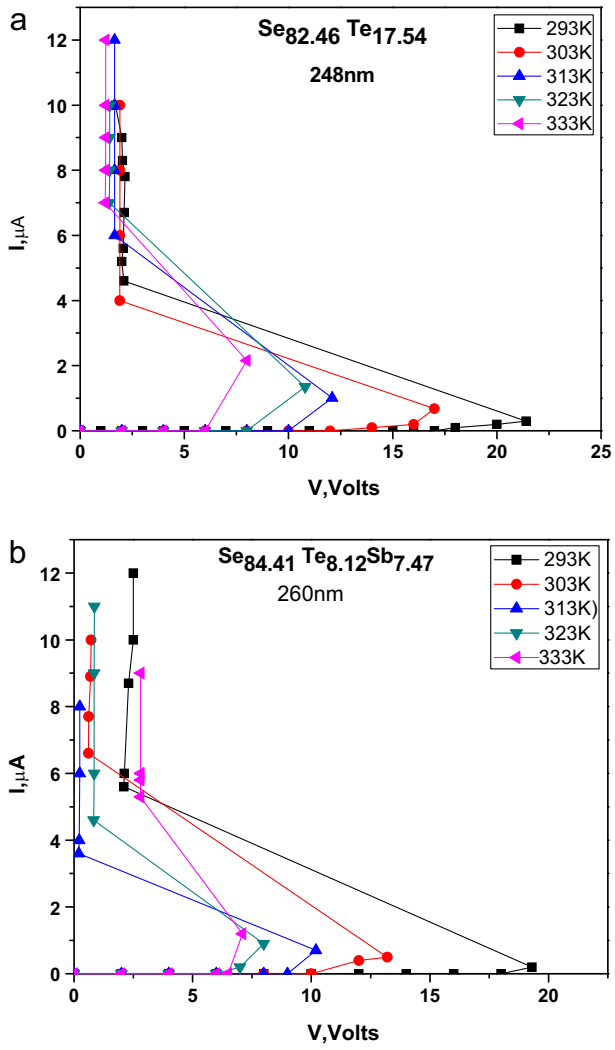

Fig. 8. (a and b) *I–V* characteristic curves at different temperatures for one thickness for $Se_{85}Te_{15}$ and $Se_{85}Te_9Sb_6$ film.

of $\bar{V}_{th}$ due to the increase of the concentration of the weaker bond energy Sb–Sb bonds in the considered system as mentioned above.

3.3.3. Temperature dependence of the threshold voltage $\bar{V}_{th}$

Fig. 8a and b depicts the temperature dependence *I–V* characteristic curves for $Se_{82.46}Te_{17.54}$and $Se_{84.41}Te_{8.12}Sb_{7.47}$ films as a representative examples. It is clear that $\bar{V}_{th}$ decreases with *T* in the investigated range. The same behavior obtained for all films of the other compositions. The obtained relations agree with those obtained before for other amorphous materials [9,10,39]. If *T* increases, the thermal energy required for the transformation of the channel material (filament) from amorphous to crystalline state will be lower. Therefore, the magnitude of $\bar{V}_{th}$ decreases with increasing temperature [35].

Fig. 9a, b and c shows ln $\bar{V}_{th}$ versus 1000/*T* for the studied compositions. The obtained relations yield straight lines indicating that $\bar{V}_{th}$ decreases exponentially with temperature in the investigated range and satisfying the following relation [9].

$$V_{th} = V_o \exp\left(\frac{\varepsilon_{V_{th}}}{\kappa_B T}\right), \quad (2)$$

where V_o is a constant, $\varepsilon_{V_{th}}$ is the threshold voltage activation energy. The values of $\varepsilon_{V_{th}}$ are calculated from the slopes of the straight lines of Fig. 9b and c. Since the obtained straight lines for each composition are parallel, indicating that the value of $\varepsilon_{V_{th}}$ is

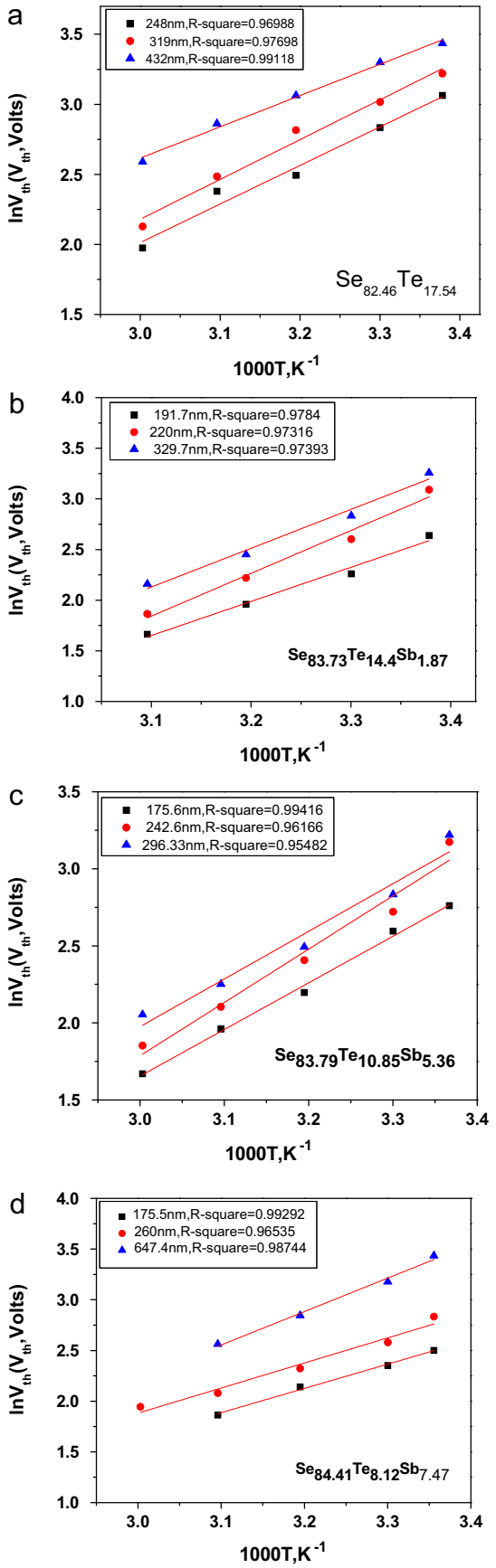

Fig. 9. (a–d) Plots of ln $\bar{V}_{th}$ versus 1000/*T* for $Se_{85}Te_{15-x}Sb_x$ film compositions.

Table 5
Values of $\Delta T_{breakdown}$ for $Se_{85}Te_{15-x}Sb_x$ films at different temperatures.

Temperature	$Se_{85}Te_{15}$	$Se_{85}Te_{13}Sb_2$	$Se_{85}Te_{11}Sb_4$	$Se_{85}Te_9Sb_6$
303	13.65	10.99	9.65	12.81
313	14.56	11.73	10.30	13.67
323	15.51	12.49	10.97	14.56
333	16.48	13.28	11.66	15.47

single value and is thickness independent. The mean value $\bar{\varepsilon}_{V_{th}}$ was calculated and given in Table 3. Thus, the ratio $\bar{\varepsilon}_{V_{th}}/\Delta E_\sigma$ was calculated using the corresponding values of ΔE_σ, are given in Table 4. It is found the ratio $\bar{\varepsilon}_{V_{th}}/E_\sigma \approx 0.5$ agrees with that obtained theoretically on the basis of the electrothermal model for the switching process [9,10] and those obtained before for other semiconducting compositions [39–42].

The observed strong temperature dependence of $\bar{V}_{th}$ can be understood in terms of the electrothermal process due to the Joule-heating effect, i.e. the temperature of the semiconducting material is raised due to Joule heating. Since the conduction process in amorphous semiconductor materials is of thermally activated type, the sample conductivity σ_{dc} is increased on heating. This allows the flow of higher current through the heated region as well as more Joule heating resulting in a further increase in the current density. Ultimately, the temperature rise will become adequate to initiate a thermal breakdown owing to the strong temperature dependence of σ_{dc}. A stationary state is reached when the heat lost by conduction from the current filament becomes equal to the Joule heat generated in that region. The heat transport equation is [9]:

$$C\left(\frac{dT}{dt}\right) = \sigma F^2 + \nabla(\Psi\,\Delta T). \tag{3}$$

The charge conservation equation is given as:

$$\frac{1}{\sigma}\frac{d\rho}{dt} = \nabla F \tag{4}$$

where ρ is the charge density, C is the heat capacity, Ψ the is thermal conductivity, F is the electric field intensity, and σ is the electrical conductivity given by Eq. (1). A general solution of these equations cannot be found with realistic boundary conditions [22].

In the case of steady state breakdown, dT/dt can be neglected for the solution of Eq. (3), then the heat conduction equation for a small difference $\Delta T = T_m - T_s$ between the temperature in the middle of the specimen T_m and that of its surface T_s becomes [9,40]:

$$8\Psi\left(\frac{\Delta T}{t^2}\right) + \sigma F^2 = 0, \tag{5}$$

where t is the film thickness, for small ΔT, the field remains uniform.

Steady state breakdown occurs when the amount of heat generated by Joule heating in the specimen of a temperature rise (ΔT) becomes larger than the extra heat flowing away or the breakdown removed by thermal conduction as a result of this temperature rise. To determine the condition for breakdown, we have to differentiate the heat balance Eq. (5) with respect to temperature and using Eq. (1) and so, the temperature difference ΔT necessary for the breakdown is given by:

$$\Delta T_{breakdown} = \frac{T^2 k_B}{\Delta E_\sigma}, \tag{6}$$

where T is the surrounding temperature of the specimen. According to Eq. (6) and using the value of ΔE_σ values of $\Delta T_{breakdown}$ were calculated for the investigated film compositions in the temperature range (297–333 K) are given in Table 5 and this agreement with those obtained for other amorphous semiconductor films [9,22,42–45]. It can be concluded that the observed memory type switching can be interpreted on the basis of the electrothermal breakdown process.

4. Conclusions

Thin films of amorphous $Se_{85}Te_{15-x}Sb_x$ (x = 0, 2, 4 and 6 at.wt%) chalcogenide glasses were prepared by thermal evaporation technique. Its amorphous nature was confirmed by the X-ray diffraction method and differential scanning calorimetry. The data obtained experimentally showed the temperature dependence for the dc electrical conductivity throughout the range (297–333 K) and thickness range (167.5–647.4 nm). This dependence is explained on the basis of the Mott and Davis model. The corresponding values of the activation energy ΔE_σ are thickness independent. The static current–voltage characteristics of these films have been found to exhibit memory type of electrical switching. It is also found that the threshold voltage increases linearly with film thickness. It decreases exponentially with temperature in the investigated range. Also, the values of the threshold voltage activation energies $\bar{\varepsilon}_{V_{th}}$, and values of the temperature difference inside and on the surface of the film were calculated. The data obtained for the switching characteristics were interpreted by the electrothermal model based on the low values of $\Delta T_{breakdown}$ and the ratio $\bar{\varepsilon}_{V_{th}}/\Delta E_\sigma$ which is found to be equal to 0.5. Moreover, the addition of Sb to $Se_{85}Te_{15-x}Sb_x$ system increases the stability in the studied system up to x = 4 at.wt% of Sb. Further increase in percentage of Sb lowers the system stability.

Appendix A. Supplementary data

Supplementary data associated with this article can be found, in the online version, at doi:10.1016/j.jallcom.2011.04.093.

References

[1] K. Homma, H.K. Henish, S.R. Ovshinsky, J. Non-Cryst. Solids 35136 (1980) 1105.
[2] S.O. Kasap, T. Wagner, V. Aiyah, O. Krylouk, A. Bekirov, L. Tichy, J. Mater. Sci. 34 (1999) 3779.
[3] G. Lucovsy, Mater. Res. Bull. 4 (1996) 213.
[4] J. Schotmiller, M. Tabak, G. Lucovsy, A. Ward, J. Non-Cryst. Solids 4 (1970) 80.
[5] E. Maruyama, Jpn. J. Appl. Phys. 21 (1982) 213.
[6] M. Horie, T. Ohno, N. Nobuuni, K. Kioyo, T. Hahizume, Tech. Digest (2001), ODS2001mci, o.37.
[7] T. Akiyama, M. Uno, H. Kituara, K. Narumi, K. Nishiuchi, N. Yamada, Jpn. J. Appl. Phys. 40 (2001) 1598.
[8] T. Ohta, J. Opto-electron. Adv. Mater. 3 (2001) 609.
[9] R.M. Mehra, R. Shyam, P.C. Mathur, J. Non-Cryst. Solids 31 (1979) 435.
[10] M.A. Afifi, N.A. Hegab, Vacuum (1997) 135.
[11] L.J. Pauling, Nature of the Chemical Bond, Cornell Univ. Press, New York, 1960.
[12] N.F. Mott, E.A. Davis, Electronic Processes in Non-Cryst. Materials, Oxford University Press, 1971, ibi, second ed. (1979).
[13] N.F. Mott, E.A. Davis, Phil. Mag. 22 (1970) 903.
[14] A. Dahshan, J. Non-Cryst. Solids 354 (2008) 3034.
[15] A. Dahshan, H.H. Amer, A.H. Moharram, A.A. Othman, Thin Solid Films 513 (2006) 369.
[16] A.H. Moharram, A.A. Othman, H.H. Amer, A. Dahshan, J. Non-Cryst. Solids 352 (2006) 2187.
[17] S.R. Ovshinsky, Phys. Rev. Lett. 21 (1968) 1450.
[18] S.J. Park, I.S. Kim, S.K. Kim, S.M. Yoon, B.G. Yuamd, S. YChoi, Semicond. Sci. Technol. 23 (2008) 105006.
[19] A.S. Glebov, in: R. Fairman, B. Ushkov (Eds.), Electronic Devices and Systems Based on Current Instability Chalcogenide Glass. III. Applications of Chalcogenide, vol. 80, Elsevier, London, 2004, pp. 1–54.
[20] N. Kalkan, S. Yildirim, K. Ulutas, D. Deger, J. Electron. Mater. 37 (2008) 157.
[21] D. Adler, Sci. Am. 36 (1977) 236.
[22] H. Fritzsche, S.R. Ovshinsky, J. Non-Cryst. Solids 4 (1970) 464.
[23] R. Rajesh, J. Philip, Semicond. Sci. Technol. 18 (2003) 133.
[24] H. Fritzsche, IBM J. Res. Dev. 13 (1969) 515.
[25] M. Dominguez, E. Marquez, P. Villares, R. Jimenez-Garay, Semicond. Sci. Technol. 3 (1988) 1106.
[26] S. Tolansky, Multiple Beam Interferometry of Surface and Films, Oxford University Press, London, New York, 1984, p. 147.
[27] J. Lucovcy, Mater. Res. Bull. 4 (1996) 505.
[28] P. Predeep, N.S. Saxena, N.B. Maharjan, Phys. Stat. Sol. (a) 189 (2002) 197.

[29] A. Giridhar, P.C.L. Narasimham, S. Mahadevan, J. Non-Cryst. Solids 43 (1981) 27.
[30] M.K. Rabinal, N. Ramesh Rao, K.S. Sangunni, Phil. Mag. 70 (1994) 89.
[31] V.K. Saraswat, V. Kishore, Deepika, N.S. Saxena, T.P. Sharma, L.I. Singh, P.K. Saraswat, Chalcogenide Lett. 5 (2008) 95–103.
[32] V.K. Saraswat, K. Singh, N.S. Saxena, V. Kishore, T.P. Sharma, P.K. Saraswat, Curr. Appl. Phys. 6 (2006) 14.
[33] K. Singh, N.S. Saxena, N.B. Maharjan, Phys. Stat. Sol. (a) 189 (2002) 197.
[34] A. Onozuka, O. Oda, J. Tsuboya, Thin Solid Films 149 (1987) 9.
[35] J. Bicerrano, S.R. Ovshinsky, J. Non-Cryst. Solids 74 (1985) 75.
[36] J.C. Phillips, J. Non-Cryt. Solids 34 (1979) 153, ibi 34 (1981) 37.
[37] M.F. Thorpe, J. Non-Cryst. Solids 57 (1983) 355.
[38] J.C. Phillips, Phys. Rev. B54 (1996) R6807.
[39] M.A. Afifi, M. Fadel, E.G. ElMetwally, A.M. Shakra, Vacuum 77 (2005) 259.
[40] M.A. Afifi, M.M. Abdel-Aziz, H.H. Labib, M. Fadel, E.G. El-Metwally, Vacuum 61 (2001) 45.
[41] M. Fadel, Vacuum 52 (1999) 277.
[42] M.M. Abdel-Aziz, Appl. Surf. Sci. 253 (2006) 2059.
[43] G.A. Denton, G.M. Friedman, J.F. Schetzina, J. Appl. Phys. 48 (1975) 3044.
[44] K. Shimakawa, Y. Inagaki, T. Arizumi, Jpn. J. Appl. Phys. 12 (1973) 1043.
[45] M.A. Afifi, H.H. Labib, A.H. Abou El-Ela, K.A. Sharaf, Appl. Phys. 46A (1988) 113.